JOURNAL OF GEOPHYSICAL RESEARCH, VOL. 113, F02019, doi:10.1029/2006JF000745, 2008

Causes of rapid mixing at a junction of two large rivers: Río Paraná and Río Paraguay, Argentina

S. N. Lane,[1] D. R. Parsons,[2] J. L. Best,[3,4,5] O. Orfeo,[6] R. A. Kostaschuk,[7] and R. J. Hardy[1]

Received 19 January 2007; revised 28 November 2007; accepted 21 February 2008; published 7 June 2008.

[1] Airborne and satellite observations show that when large rivers join they can take hundreds of kilometers to mix completely but, on occasion, may mix very rapidly. Application of established semitheoretical analyses shows that long mixing lengths should be expected. The first measurements of mixing processes at a large river junction (Río Paraná and Río Paraguay, Argentina, combined width ~2.8 km) are presented at two occasions: first when they mix in >400 km, and second when mixing is complete in only 8 km downstream of the junction. For the case of slower mixing, at-a-point surveys showed that mixing driven by turbulent shear associated with a near-vertical shear layer was restricted to close to the junction (to 0.272 multiples of the postconfluence width downstream). Transect surveys showed penetration of more turbid water from the Río Paraguay underneath the Río Paraná, but this was insufficient to promote more rapid mixing. There was no clear channel-scale circulation present and slow mixing was compounded by reverse topographic forcing on the mainstream Río Paraná side of the river. This kept more turbid water on the Río Paraguay side of the river, close to the bed. In the case of rapid mixing, we found clear channel-scale circulation. The momentum ratio between the combining flows reinforced the effects of the discordance in bed height between the tributaries at the confluence and allowed penetration of more turbid Río Paraguay water further across the channel width deeper within the flow. The importance of the interaction between momentum ratio and bed morphology at channel junctions makes mixing rates at the confluence dependent upon basin-scale hydrological response, which is more likely to differ between large confluent rivers than small rivers, as a result of the different climatic/topographic zones that they may capture.

Citation: Lane, S. N., D. R. Parsons, J. L. Best, O. Orfeo, R. A. Kostaschuk, and R. J. Hardy (2008), Causes of rapid mixing at a junction of two large rivers: Río Paraná and Río Paraguay, Argentina, *J. Geophys. Res.*, *113*, F02019, doi:10.1029/2006JF000745.

1. Introduction

[2] Field measurements and remotely sensed data show that the complete visual mixing of flows where two large rivers join commonly requires a significant river length [*Mackay*, 1970; *Krouse and Mackay*, 1971; *Matsui et al.*, 1976; *Weibezahn*, 1983; *Stallard*, 1987], and that this distance may extend to 10s or even 100s of km (Table 1). Semitheoretical analysis [e.g., *Fischer et al.*, 1979; *Rutherford*, 1994] suggests that mixing should require a significant distance downstream, because the rate of transverse diffusion will scale with W^2, where W is the width of the combined channels. However, on occasion, some large rivers can visually mix much more rapidly than this (Table 1) and our own field observations of the junction of the Río Paraná and Río Paraguay in Argentina show that while the mixing length can be >400 km (referred to herein as slow mixing), it can also be as little as ~8 km (referred to herein as rapid mixing). Research in smaller rivers has shown that near-field processes can reduce mixing lengths substantially [e.g., *Gaudet and Roy*, 1995]. The present paper begins by reviewing semitheoretical analyses of river mixing to identify the expected mixing lengths at the junction of the Río Paraná and Río Paraguay. We then present the first detailed measurements from a large river confluence in order to evaluate the influence of the near-field processes that contribute to both slow and rapid mixing.

2. Semitheoretical Analyses of River Mixing

[3] A significant body of research completed during the 1960s and 1970s developed semitheoretical models for predicting the downstream distance required for the com-

[1]Department of Geography, Durham University Science Laboratories, Durham University, Durham, UK.
[2]School of Earth and Environment, University of Leeds, Leeds, UK.
[3]Department of Geology, University of Illinois at Urbana-Champaign, Urbana, Illinois, USA.
[4]Department of Geography, University of Illinois at Urbana-Champaign, Urbana, Illinois, USA.
[5]Ven Te Chow Hydrosystems Laboratory, University of Illinois at Urbana-Champaign, Urbana, Illinois, USA.
[6]Centro de Ecología Aplicada del Litoral, Consejo Nacional de Investigaciones Cientificas y Tecnicas, Corrientes, Argentina.
[7]Department of Geography, University of Guelph, Guelph, Ontario, Canada.

0148-0227/08/2006JF000745$09.00

Table 1. A Survey of Large River Confluences, All With a Postjunction Width of Greater Than 1 km[a]

Continent	Left Tributary	Width (km)	Right Tributary	Width (km)	Postjunction Channel Width, W (km)	Mixing Length, L (km)	L:W	Comments
South America	Meta	0.7	Orinoco	1.8	1.4	7.9, >2000	5.6, >111	visual record, *Stallard* [1987]
South America	Guaviare	1.0	Orinoco	0.9	1.5	>105.9, >100	>69, >69	mixing not complete when downstream junction occurs, *Weibezahn* [1983]
South America	Amazon	3.4	Purus	1.1	2.4	14.6	6.1	...
South America	Japura	2.0	Amazon	1.4	2.9	>202.1	>70	mixing not complete when downstream junction occurs
South America	Apaporis	0.5	Japura	1.6	1.3	>102.5	>82	mixing not complete when imagery does not allow further interpretation
South America	Branco	0.9	Negro	1.6	2.4	36.2	15	...
South America	Paraguay	0.9	Paraná	2.4	3.0	>376.1, 8	>127, 3.3	visual mixing not complete when influenced by return flow from wetland, from 2004
South America	Negro	3.6	Solimoes	3.1	4.6	>121, >120	>30, >30	mixing not complete when downstream junction occurs, *Matsui et al.* [1976]
North America	Liard	0.66	Mackenzie	1.06	1.59	51.4, >320, >480	33, >202, >302	visual record longer distances revealed by isotope analysis, *Mackay* [1970], *Krouse and Mackay* [1971]
Africa	Kasai	0.9	Lukenie	0.6	1.1	>93.5	>87	mixing not complete when downstream junction occurs
Africa	Benue	1.1	Niger	1.0	1.4	103.9	76	...
Asia	Yenesy	1.3	Velmo	0.8	1.9	141.3	75	...
Asia	Lena	0.9	Olekma	0.9	1.4	159.0	111	...
Asia	Izhma	0.6	Pechora	1.6	2.7	>192.2	>72	mixing not complete when downstream junction occurs

[a]The mixing length was measured visually from satellite imagery and does not represent the actual mixing length, only that at which the two tributary flows are still visually distinguishable. This restricts attention to mixing at junctions with visually different waters. In some cases, the mixing length was interrupted by a later junction, and mixing length was only measured up to this point. Where field measurements of the same junction are available, a second distance is provided. The first value is the remotely sensed distance. The second and third values are the field-measured data from the respective sources given in the last column. We observed complete mixing in the Río Paraguay-Paraná confluence in 2004, and this is indicated. Left is defined as looking downstream.

plete transverse mixing of two confluent rivers (the transverse mixing distance, L_z). For a conservative tracer that has become vertically well mixed close to the source (i.e., in the near field), the analysis becomes two-dimensional (2-D) [*Rutherford*, 1994]. If the source is steady, and hence the longitudinal dispersion term negligible, the depth-averaged cross-stream (y) velocity is zero, the downstream (x) mean depth, depth-averaged velocity (U) and transverse dispersion coefficient (k_y) are constant, and $k_y \gg \varepsilon\, y$, the turbulent diffusion coefficient, then:

$$U\frac{\partial c}{\partial x} = k_y \frac{\partial^2 c}{\partial y^2}, \tag{1}$$

where c is the tracer concentration. This is the constant-coefficient model of transverse mixing. Solution of this equation for the special case of the junction of two rivers (i.e., $\partial c/\partial y = 0$ at $y = 0$ and $y = W$) is given by *Fischer et al.* [1979]. For the case where the mixing interface is at approximately $y = 0.25W$, as in the river junction studied here, and with mixing complete to within ±5%, then:

$$L_z \approx 0.18\frac{UW^2}{k_y}. \tag{2}$$

Equation (2) allows determination of the effective value of k_y required to reproduce the observed L_z, albeit with some uncertainty given that the data in Table 1 are based upon visual data. For the junction of the Río Paraná and Río Paraguay, $k_y \approx 5.6\ \mathrm{m^2\ s^{-1}}$ for the slower mixing case (2005) and $k_y \approx 266.0\ \mathrm{m^2\ s^{-1}}$ for the more rapid mixing case (2004). It is normal to nondimensionalize k_y by dividing by dU^*, where U^* is the shear velocity, $(gdS)^{0.5}$, and S is reach slope (0.00005 for the Paraná): for the slower mixing case, $k_y/dU^* = 11.8$ and for the more rapid mixing case $k_y/dU^* = 648.8$. Comparison of these values with established estimates of k_y/dU^* [e.g., *Fischer et al.*, 1979; *Rutherford*, 1994] suggests that the slower mixing case is close to the range of experimental results for curved channels, $1 < k_y/dU^* < 3$ [*Rutherford*, 1994], whereas the rapid mixing case is 2 orders of magnitude higher than any values reported by *Rutherford* [1994].

[4] The above analysis determines the effective value of k_y required in (2) in order to reproduce the visually observed mixing length, with this distance thus being influenced by local mixing processes associated with flow at the junction (the near field) and mixing associated with far-field processes. Research in small rivers has shown that three primary flow mechanisms contribute to near-field mixing at river confluences: (1) shear between the confluent flows [*Best*, 1987], which may lead to the formation of two-dimensional vortices with near-vertical axes [*Brown and Roshko*, 1974; *Rogers and Moser*, 1992] that translate and merge as they are advected and stretched downstream [*Winant and Browand*, 1974; *Sukhodolov and Rhoads*, 2001]; (2) helical motions (secondary circulation) associat-

Figure 1. The confluence of the Río Paraná and Río Paraguay, northern Argentina. (a) Satellite image taken during a period of slow mixing in 2005, with Río Paraná on the right (dark blue) and Río Paraguay on the left (light blue). (b) Inset photograph showing the case of rapid mixing in 2004 viewed looking upstream; the associated mixing interface from 2004 is superimposed as a white line on the satellite image in Figure 1a. (c) Illustration of the coordinate system used in the study, viewed looking downstream; also note the nature of the vortices that are visually apparent along the mixing interface.

ed with curved channels, produced by the variation with depth in the magnitude of transverse velocity deriving from bed friction effects, curvature-induced pressure gradients and bed topography [*Mosley*, 1976; *Best*, 1988; *Rhoads and Kenworthy*, 1995, 1998; *Rhoads*, 1996; *Bradbrook et al.*, 2000]; and (3) the effects of a difference in bed elevation (discordance) between the two confluent channels [*Best and Roy*, 1991; *Biron et al.*, 1993, 1996; *Gaudet and Roy*, 1995; *McLelland et al.*, 1996], which generates a zone of low or negative dynamic pressure in the lee of the shallower channel [*Bradbrook et al.*, 2000], and which may drive the upwelling of fluid from one channel into the waters of the other confluent channel [*Best and Roy*, 1991]. Each of these mechanisms may therefore contribute to mixing of the two confluent rivers. Two-dimensional vortices, with near-vertical axes, may lead to substantial lateral transfers of fluid between the two combining flows, although observations in small channels suggest that this only results in mixing as long as the shear between the two flows is maintained [*Sukhodolov and Rhoads*, 2001; *Rhoads and Sukhodolov*, 2001]. Helical circulation may result in substantial mixing if the secondary flow cells merge into a single, channel-scale, helical cell [*Rhoads and Sukhodolov*, 2001]. The upwelling of water at discordant bed junctions has been shown to reduce the downstream distance required for complete mixing from approximately 100 multiples of channel width (W) to as little as $25W$ in small rivers ($W <$ 10 m) [*Gaudet and Roy*, 1995].

[5] All of these speculations concerning the nature of near-field mixing at open-channel confluences have been based upon field, laboratory or computational studies of rivers that have small channel widths (<10 m). The analysis of effective k_y values above, combined with the demonstrated importance of near-field processes for mixing in small rivers, leads to two related questions: (1) For the case of slower mixing, why do near-field processes have so little effect, resulting in an effective k_y value that has a similar order of magnitude to that expected for far-field mixing alone? (2) In what ways are the near-field processes so different, in the same river, such that the effective k_y value is 2 orders of magnitude greater at one measurement period than at a another?

3. Field Site and Methodology

[6] To address these questions, we have measured morphology, flow and sediment dynamics at the confluence of the Río Paraná (basin area to Paraná-Paraguay junction,

Table 2. Characteristics of the Río Paraguay and Río Paraná in 2004 and 2005

Date	Río Paraguay Discharge (m^3s^{-1})	Río Paraná Discharge (m^3s^{-1})	Río Paraguay Suspended Sediment Concentration (mgL^{-1})	Río Paraná Suspended Sediment Concentration (mgL^{-1})	Río Paraguay Fluid Density Corrected for Suspended Sediment (kgm^{-3})	Río Paraná Fluid Density Corrected for Suspended Sediment (kgm^{-3})	Momentum Ratio Assuming No Sediment Effect, Paraná: Paraguay	Momentum Ratio Including Sediment Effect, Paraná: Paraguay
February 2004	4,800	10,500	1,100	40	997.19	996.53	1.795	1.792
May 2005	3,500	12,500	600	40	996.87	996.53	3.601	3.598

1,510,000 km^2) and Río Paraguay (basin area to Paraná-Paraguay junction, 1,095,000 km^2), in NW Argentina (Figure 1). We surveyed the rivers in February 2004, when they mixed completely in $\sim 3.3W$, and again in May 2005, when they mixed in $\sim 127W$ (see Table 2 for flow characteristics). The postjunction river channel is 2.8 km wide (W) and has a mean depth (d) of ~6.0 m, giving a W:d ratio of ~470, or 1 to 2 orders of magnitude larger than that typical of small river junctions. The morphology of the junction (Figure 2) shows that the bed elevations at the junction are discordant [*Kennedy*, 1984], with the Río Paraná entering the junction with a bottom elevation about 10–15 m above the bed of the Río Paraguay. Upstream of the junction, the Río Paraguay becomes confined by a bedrock constriction and is significantly over deepened as the flows combine.

[7] The momentum ratio (M_r) between the two rivers can be defined as:

$$M_r = \rho_{PA} Q_{PA} U_{PA} / \rho_{PY} Q_{PY} U_{PY}, \quad (3)$$

where: ρ is density; Q is discharge; U is section-averaged downstream velocity; and the subscripts PA and PY denote the Río Paraná and Río Paraguay, respectively. In 2005, M_r = 3.60, if it is assumed that the densities of the Río Paraná and Río Paraguay fluid are the same. In practice, the Paraguay normally carries a significant fine sediment load, and so Table 2 also shows the fluid densities (at 27°C) corrected for the effects of vertically averaged suspended sediment concentration, which results in only very small changes in the momentum ratio.

[8] Two types of data were collected in May 2005: (1) at-a-point, fixed mooring measurements for 90–120 min at various distances downstream along the mixing interface and (2) additional, moving vessel, transects to assist in the interpretation of these at-a-point data. Data are also reported that were collected in February 2004, when the mixing distance was considerably less (Table 1) and the momentum ratio lower (M_r = 1.80). The 2004 field season was designed to focus upon quantifying the junction morphology and general flow structure, rather than mixing in detail, and thus no systematic at-a-point fixed mooring data were taken. However, the section transects surveyed in February 2004 are spatially coincident with those taken in May 2005 and this facilitates the comparison of a slow mixing field case (measurements in May 2005) with a rapid mixing field season (measurements in February 2004).

[9] Measurements of the 3-D confluence bathymetry and 3-D flow structure were made from a small vessel using a RESON SeaBat 8101 Multibeam Echo Sounder (MBES) and an RD Instruments RioGrande 600 kHz acoustic Doppler current profiler (ADCP). Both instruments were located together spatially and temporally using a Leica differential global positioning system (DGPS) in real time kinematic (RTK) mode, which produced an accuracy in relative position (DGPS base station to mobile rover) of ±0.02 m and ±0.03 m in the horizontal and vertical positions, respectively. The vessel velocity and track position along predetermined survey lines were monitored online and held as constant as possible during surveying, with the vessel velocity being ~1 ms^{-1}.

[10] The MBES provided information on the river bed morphology at a centimetric resolution and millimetric precision over scales from ripples superimposed on dunes to the entire river reach. MBES measurements were taken for the whole confluence area. The RESON SeaBat 8101 MBES employed was a 240 kHz system, which measured the relative water depth along 101 beams across a wide swath (210°) perpendicular to the track of the survey vessel. A combined motion and gyro sensor (a TSS Ltd. Meridian Attitude and Heading Reference System (MAHRS)) was used to provide full 3-D motion and orientation data for the MBES processing, and the DGPS was set to output both RTK position and a pulse per second (PPS), which was used to remove all latency from the MBES setup. Postprocessing of the MBES data was achieved using Caris HIPS to produce the final gridded bathymetric surface of the whole confluence area (Figure 2).

[11] These MBES bed surveys were accompanied by three-dimensional flow measurements using the ADCP both along predetermined transects and from at-a-point, fixed moored positions. The backscattered signal was split into equally spaced 0.5 m vertical bins in 2005. In 2004, in situ tests showed that the higher suspended sediment concentration (Table 2) necessitated use of 1.0 m vertical bins so as to overcome some of the impacts of signal attenuation. Since all velocities measured by the ADCP were relative to the ADCP, and hence include both flow and vessel velocity, the measured ADCP velocities were corrected for the vessel motion by removing the DGPS-derived vessel velocity, thereby producing measurements of the three-dimensional flow velocity [cf. *Yorke and Oberg*, 2002; *Muste et al.*, 2004]. In order to reduce potential errors in flow velocity, a five profile (or ensemble) running average was used along each individual section transect to determine the final 3-D velocity profiles. Such spatial and temporal averaging across each transect was used in an attempt to remove some of the higher-frequency turbulence and DGPS positional variations from the final ADCP transect results. Although

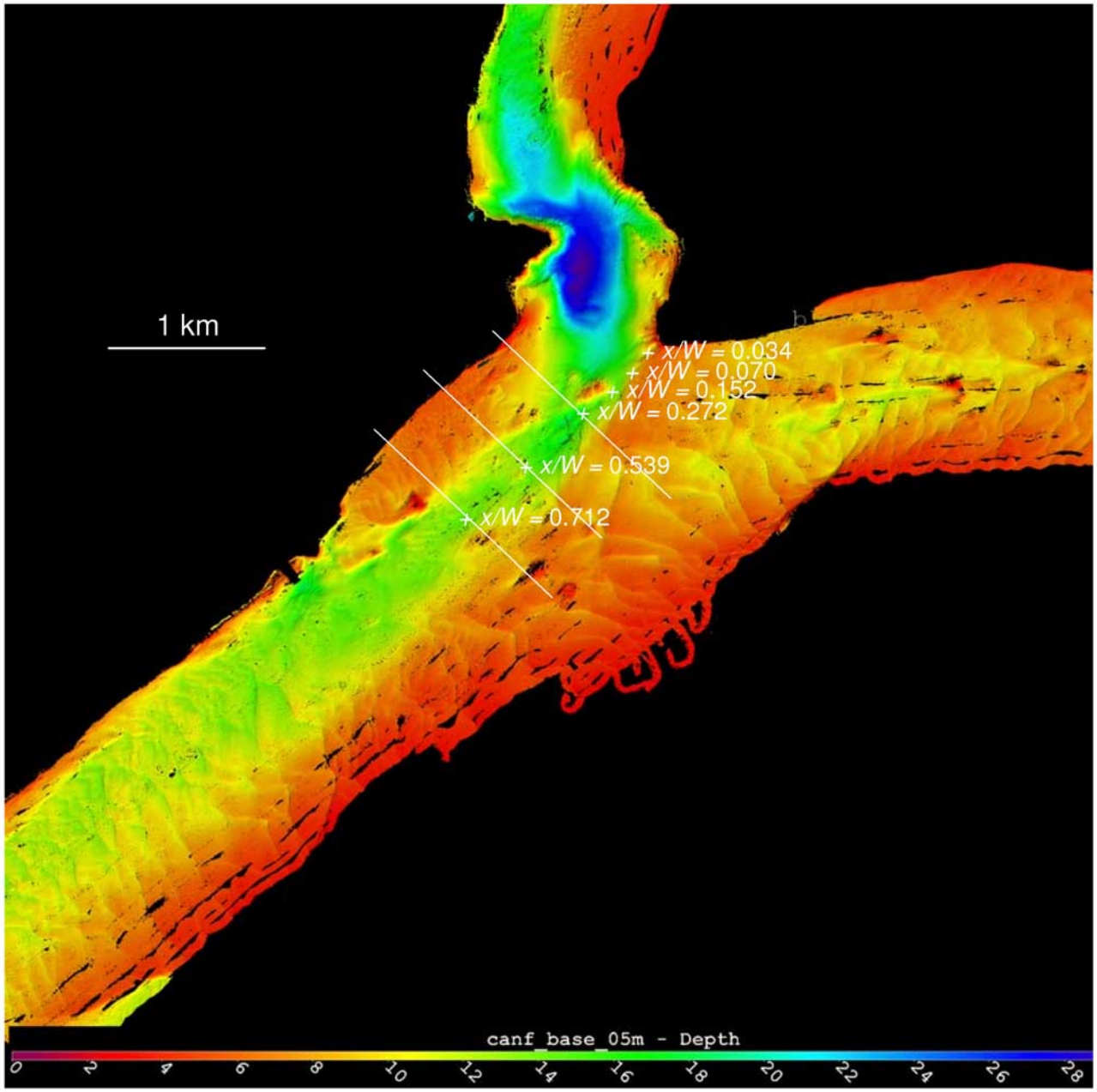

Figure 2. Confluence morphology as measured by multibeam echo sounding. Crosses depict location of fixed mooring locations in 2005, while lines show transects surveyed in both 2004 and 2005.

using only one transect per section may have some drawbacks with regards to reducing spatial resolution and obtaining fully time-averaged results [e.g., *Muste et al.*, 2004], *Dinehart and Burau* [2005] and *Szupiany et al.* [2007] show that single transects, with suitable along-track averaging intervals, are able to describe adequately the flow through a cross section, including the larger-scale secondary flow fields. Moreover, because of the temporal scale of the low-frequency flow variations associated with the velocity shear within the confluence, obtaining fully time-averaged results at this site is problematic. For the at-a-point locations, the ADCP time series data was not subject to any averaging as the errors associated with velocity measurement due to vessel movement (maximum horizontal variations in complete fixed point time series were ~5 m) and Doppler noise were far less when the vessel motions were very small compared with flow velocity.

[12] The ADCP also provided a measure of echo backscatter intensity (in decibels), on the basis of the received signal strength of the returning echo from scattering particles within the water column for each of the bins in each vertical profile. Beyond the near-zone distance (the distance from the transducer where the beam topology transforms from cylindrical to conical), the echo backscatter values require correction for transmitted power, beam spreading, and sound absorption. As beam spreading varies linearly with depth, with a fixed system frequency and constant transducer power, sound absorption is thus essentially an

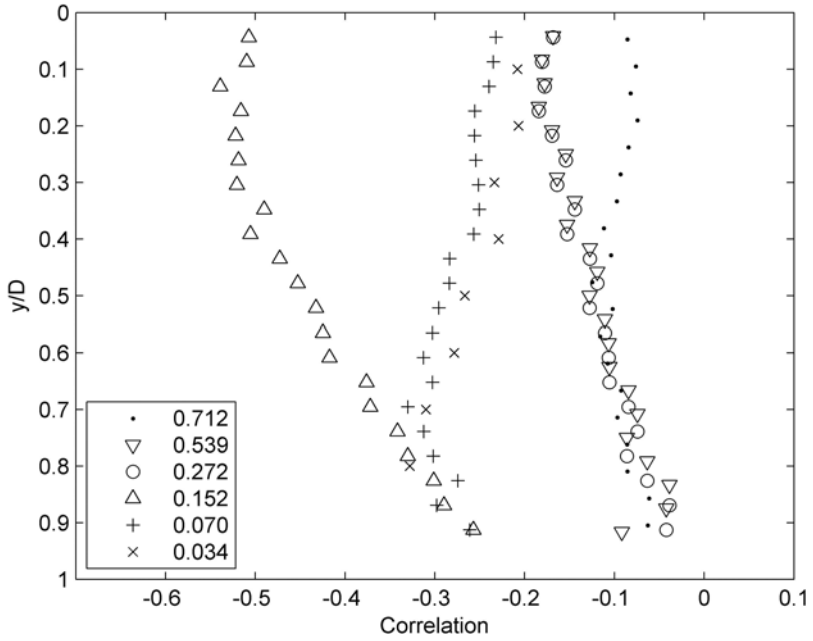

Figure 3. Correlation of the deviatoric values of sediment concentration and the lateral component of velocity (c' and v', respectively) plotted against depth below the surface (y/D, 0, surface, 1 bed), with their distance downstream expressed as multiples of the postjunction width (x/W in legend). Data are for 2005 when mixing was slow.

indication of the properties of the water column and can therefore be related to the major cause of absorption, namely the suspended sediment concentration. Direct point samples of suspended sediment concentration were obtained with a Rutner sampler and used to calibrate the ADCP acoustic backscatter values. In 2005, this relationship allowed use of the ADCP backscatter signal for measurement of suspended sediment throughout the vertical profiles along each of the transects and through time at the fixed positions. This proved more difficult for the 2004 data as a result of the high rates of signal attenuation, and thus we only use backscatter data for the 2005 results in this paper.

[13] For the transect data from both years, the flow direction was defined by plane rotation during postprocessing to give no net cross-stream discharge [*Lane et al.*, 2000]. For the 2005 data, the suspended sediment time series and transects from the ADCP were analyzed by labeling them according to the cumulative frequency distribution of all suspended sediment observations for each transect. This is done on a by-transect basis as a result of downstream changes in the maximum suspended sediment concentration. We use three labels: 1.0, 0.67 and 0.33, with the concentration boundaries set at 67% and 33% of the distribution. For the 2005 transect data, the rotated downstream and lateral velocities were combined with suspended sediment data to determine the downstream and lateral suspended sediment fluxes. For the at-a-point data, we undertook a classical Reynolds decomposition of each velocity signal *vi* ($vi = u$ for downstream, v for lateral, w for vertical, see Figure 1) and concentration signal (c) into their mean (overbar) and deviatoric (primed) components

$$v_i = \overline{v_i} + v_i' \qquad c = \overline{c} + c'. \tag{4}$$

Through determination of the $v_i c$ product and integrating this through both time and the flow depth at each measurement point, the associated suspended sediment flux was determined.

4. Results

[14] Here, we explore two mixing processes: (1) that associated with shear-driven turbulence, using data acquired during slow mixing and (2) that associated with channel-scale circulation, using data acquired during both slow mixing and rapid mixing.

4.1. Mixing Arising From Shear Between Confluent Rivers: Case of Slow Mixing

[15] Figure 3 quantifies the strength of association between velocity variations and fluctuations in suspended sediment concentration, recorded during the at-a-point monitoring in 2005, when mixing was slow. The negative correlations at $x/W = 0.034$ and 0.070 indicate transport of higher turbidity water from the Río Paraguay toward the Río Paraná and/or lower turbidity water from the Río Paraná moving toward the Río Paraguay. At $x/W = 0.152$, these negative correlations have become particularly strong (Figure 3), notably at the surface. By $x/W = 0.272$, 0.539, and 0.712, the negative correlation between v' and c' has become much reduced, and is only really significant at the surface, with the surface correlations being further reduced at the latter location. Figure 4a shows the associated lateral fluxes, by integrating $v'c'$ through the vertical. Lateral flux declines rapidly between $x/W = 0.152$ and $x/W = 0.272$. The exceedance probability plot (Figure 4b) shows almost no change in the distribution of suspended sediment concentration between $x/W = 0.272$ and $x/W = 0.712$. As the

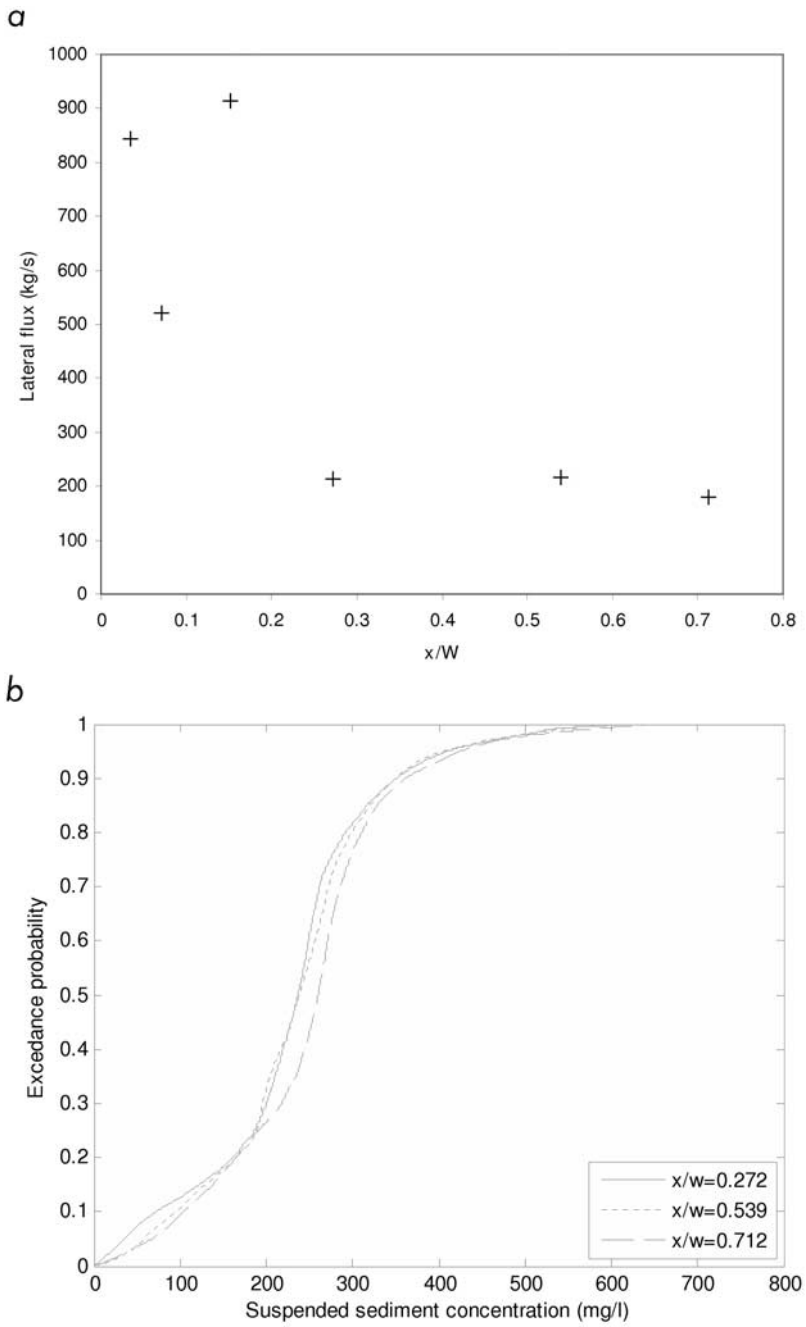

Figure 4. (a) Lateral flux of sediment from the Río Paraguay river toward the Río Paraná plotted as a function of distance downstream (x/W) and (b) exceedance probability plots to show the distribution of suspended sediment concentrations for x/W = 0.272, 0.539, and 0.712.

distribution is maintained, the decline in $v'c'$ must be due to a decrease in the intensity of shear-induced turbulent mixing rather than a decline in lateral suspended sediment concentrations. Thus, the rapid lateral mixing process induced by strong shear at the river confluence has almost disappeared within 0.272 multiples of the postconfluence width.

4.2. Mixing Arising From Channel-Scale Circulation: Case of Slow Mixing

[16] Transect surveys of velocity and suspended sediment concentration obtained in May 2005 show that shear-driven mixing processes are not enhanced by channel-scale processes. Three transects are chosen for analysis here, corresponding to x/W = 0.272, 0.539, and 0.712, respectively (Figure 2). Figures 5a–5f show a core of high velocity flow at x/W = 0.272, extending from 850 m to 1500 m along the transect. To the left of 1150 m, there is a zone of flow moving toward the Río Paraguay (positive values, Figure 5b) that is also associated with a region of turbid water (Figure 5d), which extends through the vertical to the surface. This turbid water is also associated with a zone of upwelling (positive vertical velocity, Figure 5c). To the right hand side of this feature (1150 to 1400 m) in the

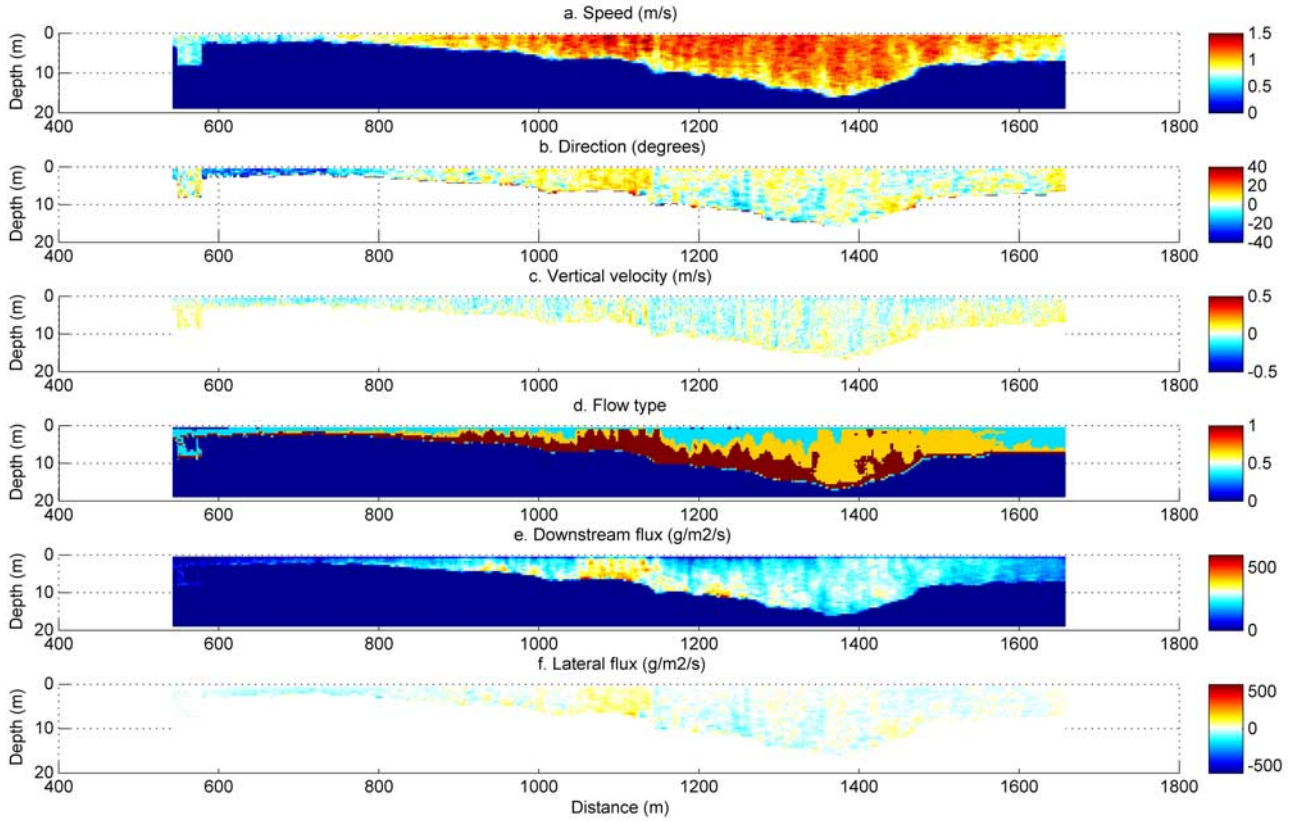

Figure 5. Transect surveys for 2005 of (a, g, and m) flow speed, (b, h, and n) flow direction (with respect to transects oriented to give zero net cross-stream discharge, negative toward the Río Paraná, positive toward the Río Paraguay), (c, i, and o) vertical velocity (positive upward), (d, j, and p) flow type (1, Río Paraguay; 0.33, Río Paraná; 0.67, intermediate, 0.00 bed), (e, k, and q) downstream sediment flux, and (f, l, and r) lateral sediment flux (in v, negative toward the Río Paraná and positive toward the Río Paraguay). Data are presented for three transects (see Figure 2 for locations), i.e., $x/W = 0.272$ (Figures 5a–5f), $x/W = 0.539$ (Figures 5g–5l), and $x/W = 0.712$ (Figures 5m–5r). Each cross section is viewed looking downstream, i.e., distance is measured from the true left. The line on Figure 5m indicates the possible angled shear layer.

deepest part of the transect, the flow generally moves toward the Río Paraguay at the surface (positive directions, Figure 5b), and toward the Río Paraná at the bed (negative directions), but neither the near-bed nor near-surface flow are continuous over any great distance, and become less coherent beyond 1400 m to the end of the transect. To the left hand side of 1150 m, the flow shallows significantly. From 800 m, where the section crosses the downstream extension of the step in the bed morphology of the Río Paraná (Figure 2), to 1150 m, the flow is generally toward the Río Paraguay, aided by the direction of the bed gradient. This effect may explain the upwelling and surfacing of the more turbid water at 1150 m. Flow moving down the face of the step, from the Río Paraná to the Río Paraguay (between 800 m and 1150 m) meets flow that is, at least at the bed, moving generally from the Río Paraguay to the Río Paraná, resulting in upwelling of turbid water to the surface. Thus, large-scale topographic forcing associated with large-scale channel morphology, such as the downstream extension of the morphological step in this confluence, appears to prevent the extension of turbid water at depth from the Río Paraguay into the Río Paraná, leading to a lack of mixing between the two flows.

[17] Figure 4 shows that the vertically integrated advective flux at $x/W = 0.272$ was much lower than closer to the junction corner. The magnitudes of the downstream and lateral flux are plotted in Figures 5a(v) and 5a(vi), and show that the downstream flux that is associated with the region of high turbidity, and that extends through the flow depth at 1150 m, is both high and greater than in the adjacent waters. This region also results in a notable lateral flux (Figure 5f) toward the Río Paraguay (positive values). Figure 6 plots the cross-stream variation in the vertically integrated fluxes for both the downstream and lateral directions for the transects at $x/W = 0.272$, 0.539, and 0.712. Despite the vertical suspended sediment concentrations that appear to dominate some parts of the patterns of flow type (Figures 5d, 5j, and 5p), there are clear patterns in both the downstream and lateral fluxes. Generally, for each of the transects, the downstream sediment flux is approximately one to 2 orders of magnitude greater than the lateral flux, with the lateral flux having phases of being both negative (toward the Río Paraná) and positive (toward the Río Paraguay). The major zone of positive flux at $x/W = 0.272$ is associated with the high turbidity at 1150 m described above, although the lateral flux is generally negative to the left side of 800 m,

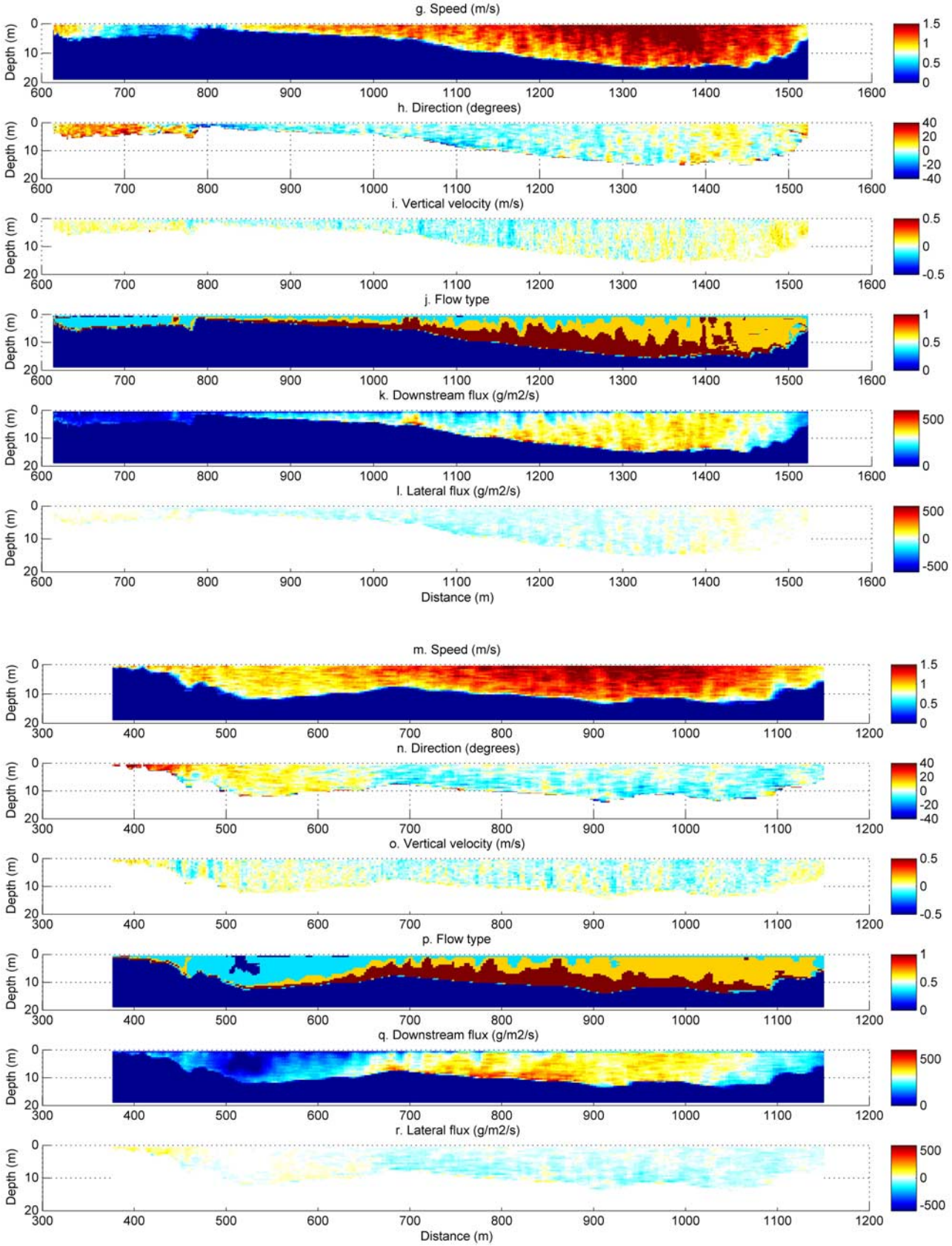

Figure 5. (continued)

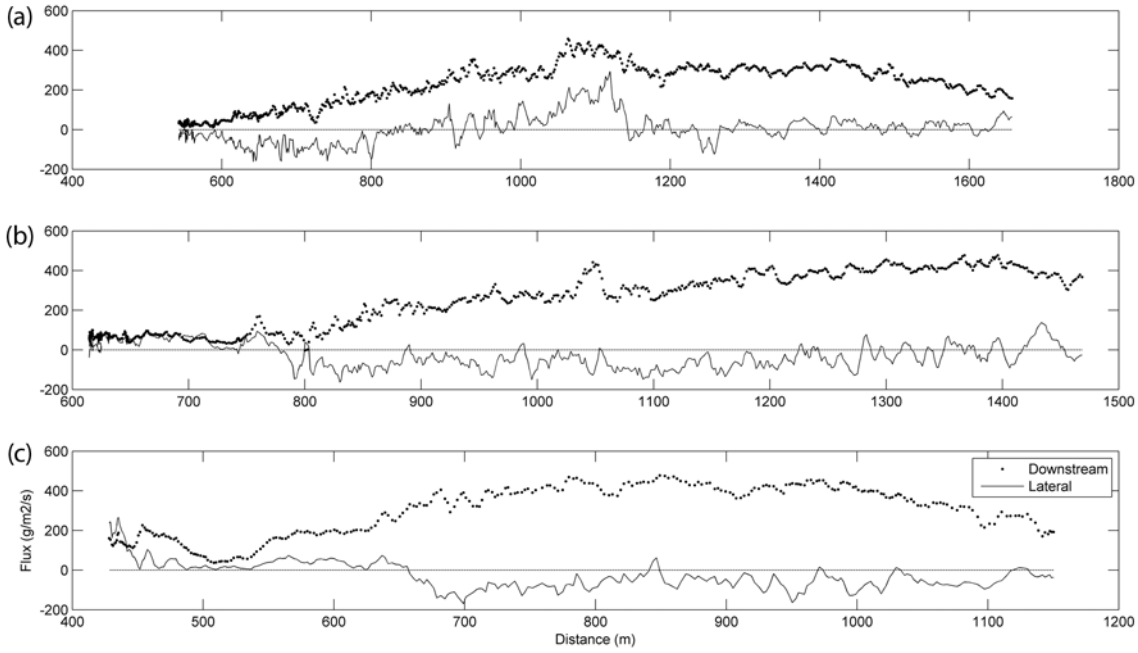

Figure 6. Vertically averaged downstream and lateral sediment flux for (a) $x/W = 0.272$, (b) 0.539, and (c) 0.712 for 2005. Negative lateral flux indicates flux toward the Río Paraná.

indicative of flux from the Río Paraguay to the Río Paraná. The laterally integrated lateral flux is slightly negative, at 2,600 kgs^{-1}, indicating a very small, but net flux from the Río Paraguay toward the Río Paraná. The value of laterally integrated lateral flux is almost 2 orders of magnitude smaller than the laterally integrated downstream flux of 158,900 kgs^{-1}.

[18] At $x/W = 0.539$ (Figures 5g–5l) there is some acceleration of flow as compared to $x/W = 0.272$, and the patterns in flow direction have also changed. The extension of the morphological step in the Río Paraná on the left side of the channel is notable when compared with transect $x/W = 0.272$, with a high point in its elevation at 800 m at $x/W = 0.539$, with the flow appearing to converge on top of the step (Figure 5h). To the left of the step, flow moves slowly and has a rightward (positive) direction toward the Río Paraguay. To the right of the top of the step to ~1350 m along the transect, there is the expected leftward movement of flow toward the Río Paraná (negative directions), although after 1350 m the flow pattern is less coherent with flow moving right, from the Río Paraná toward the Río Paraguay (1350 to 1450 m), followed by a region of leftward directed flow (Figure 5h). In the $x/W = 0.539$ transect, the turbid Río Paraguay water is generally below the surface (Figure 5j), particularly to the left of 1350 m, although small pockets of more turbid water extend throughout the flow depth, notably again as the morphological step shallows at 1050 m. The patterns of downstream flux (Figure 5k) reveal that the main flux is associated with higher concentration Río Paraguay water below the surface, mostly to the right side of 1200 m. Lateral flux in the transect (Figure 5l) is mainly associated with movement from the Río Paraguay toward the Río Paraná (negative values). The vertically integrated lateral flux (Figure 6) is toward the Río Paraguay (i.e., positive) to the left of the top of the step at 800 m and largely negative to the right, showing the general trend of flux from the Río Paraguay toward the Río Paraná. However, the fluxes are generally small, and large-scale topographic forcing by the top of the step may be contributing to keeping the more turbid water on the Río Paraguay side of the channel. The zones of more turbid water moving toward the Río Paraguay are sufficient for the vertically integrated lateral flux to be back toward the Río Paraguay for short distances (Figure 6), but the laterally integrated lateral flux is strongly toward the Río Paraná with a value of 11,600 kgs^{-1}. The downstream flux was 173,200 kgs^{-1}, higher than at $x/W = 0.272$, illustrating the flow acceleration described above.

[19] At $x/W = 0.712$, the overall flow velocity has reduced slightly (Figure 5m) and the extension of the step, whose effects are clearly apparent in Figures 5a–5l, is now significantly lower in elevation, with its highest point at ~680 m. This point marks a clear difference in flow direction, indicative of converging flow, with flow moving toward the Río Paraguay on the left hand side and toward the Río Paraná on the right side of the top of the step (Figure 5n). The zone of flow moving toward the Río Paraná extends further toward the Río Paraná at the surface, creating what appears to be an angled shear layer (Figures 5m and 5n, 600–700 m), although it is not clear that the velocity differential along this interface is sufficient for this to be a true "shear" layer. Vertical velocities on the Río Paraná side of this oblique flow boundary are generally upward and those on the Río Paraguay side are generally more downward, although the magnitudes are generally very low. This vertical velocity structure probably explains why the zone of high turbidity remains confined to the bed, and a zone of clear Río Paraná water remains distinct to the left of the top of the step (680 m). When compared with $x/W = 0.539$, on the right hand side of the top of the step, there are fewer

columns of water moving toward the Río Paraná. Indeed, overall at $x/W = 0.712$ there is a weak tendency for flow to move toward the Río Paraguay at the surface and toward the Río Paraná at the bed, but this is less coherent than at $x/W = 0.539$. These patterns of turbidity are also reflected in the downstream flux (Figure 6), which is higher at $x/W = 0.712$ than at either $x/W = 0.272$ or 0.539, and is dominated by the Río Paraguay side of the river once more. Similar to the flow direction, the lateral flux is predominantly toward the Río Paraná to the right of 650 m (negative), and toward the Río Paraguay to the left (positive) of 650 m. These values are sufficient to result in the vertically integrated lateral fluxes being positive to the left of the step and negative to the right (Figure 6). The laterally integrated flux was 1,100 kgs^{-1} toward the Paraná.

[20] The above analysis suggests that there are three processes controlling the mixing downstream of $x/W = 0.152$, where the at-a-point observations of sediment concentration suggest dramatically lower shear-related mixing (Figure 4). The first process is essentially a net result of flow structures formed either in the near-confluence zone or associated with turbulent suspension events linked to form roughness, and the influence of the morphological step, at the bed. These structures take the form of columns of more turbid water that extend toward the flow surface and tend to result in high-magnitude fluxes of turbid water in the downstream direction ((Figures 5bv) and (5cv)). However, since these structures were sometimes associated with water moving from the Río Paraguay to the Río Paraná and vice versa, they did not have a particularly large, sustained effect on mixing. Second, away from the influence of the extension of the morphological step on the left hand side of the channel, there was generally a zone of turbid, near-bed flow moving predominantly toward the Río Paraná and a region of clearer surface flow moving toward the Río Paraguay, although the latter was sometimes disrupted by the features described above. These movements of fluid result in a tendency for a net lateral flux of turbid water toward the Río Paraná from the Río Paraguay, although this was much smaller than the magnitude of the laterally integrated downstream flux in all cases. Third, this second process did not extend throughout the whole postconfluence channel, primarily as a result of extension of the step. At the upstream transect ($x/W = 0.272$), the edge of the step formed the bar top, generating flow divergence, and caused turbid fluid to move back toward the Río Paraguay throughout the full flow depth. Further downstream ($x/W = 0.539$), there was a transition toward flow convergence on the top of the step throughout the flow depth (Figures 5g–5l), which prevented further movement of the near-bed turbid water toward the Río Paraná, perhaps exacerbated by the reverse bed slope on the right hand side of the step top. As the flow depth over the step increased with distance downstream (to $x/W = 0.712$), this flow convergence throughout the flow depth continued, forming an angled boundary between water moving toward the Río Paraguay at the surface and toward the Río Paraná nearer the bed, but with no clear evidence of the velocity shear that would be required to enhance mixing further. These observations suggest the significant influence of strong topographic forcing of the flow on the left hand side of the postjunction zone, possibly aided by the effects of form roughness upon transmission of bed effects through the flow depth. Such processes thus slow the transfer of more turbid water toward the Río Paraná. Turbulent ejections of near-bed turbid water toward the surface, associated with the form roughness, could counter this effect, but do not appear to do so sufficiently and thus full width scale mixing of the two flows is not enhanced by near-field processes.

4.3. Mixing Arising From Channel-Scale Lateral Transfers: Case of Rapid Mixing

[21] The data collected in May 2005, and discussed above, were associated with a period when the visual mixing length was 100 s of multiples of the postconfluence width. We were able to compare these results with data collected during February 2004 when the river mixed within a very short distance (Figure 1b), of approximately 8 multiples of the junction width (Table 1). The principal differences in flow between 2004 and 2005 are (Table 2): (1) a slightly lower combined discharge in 2004 (16,000 $m^3\ s^{-1}$ in 2005, 15,300 $m^3\ s^{-1}$ in 2004); (2) a higher relative discharge in the Río Paraguay, which produced a momentum ratio close to half of that in 2005; and (3) a higher suspended sediment concentration in the Río Paraguay in 2004 (600 mg L^{-1} in 2005, 1,100 mg L^{-1} in 2004), which equates to density ratios (Paraguay: Paraná) of 1.00066 in 2004 and 1.00035 in 2005. As noted above, the main problem with sampling in 2004 was that the increase in the suspended sediment concentration made it difficult to calibrate the ADCP acoustic backscatter with sediment concentration. Thus, reliable estimates of suspended sediment concentration throughout the flow depth and calculations of the downstream and lateral flux (e.g., Figure 5) were not possible. However, it was possible to determine the stream-wise and vertical velocities, together with flow direction, for the same transects reported above: $x/W = 0.272$, 0.539, and 0.712 (Figure 7) for a case when it was clear that visual mixing was complete in a very short distance downstream (Figure 1b). This rapid mixing case reveals a dramatic difference in the nature of flow in 2004 as compared with 2005. At all three transects, there is the presence of much larger-scale and more coherent flow patterns, with flow at the bed moving toward the Río Paraná and flow at the surface moving toward the Río Paraguay. In the corresponding transects from May 2005, when mixing was slow, there was only evidence of surface flow toward the Río Paraguay at $x/W = 0.272$, and this was spatially discontinuous. In 2004 at all three transects, flow is consistently moves toward the Río Paraná at the bed and toward the Río Paraguay at the surface, with the Río Paraná directed near-bed flow having a lower velocity than the near-surface flow moving toward the Río Paraguay (Figure 7). The result of this is a marked velocity differential, and hence a stronger shear than in 2005, although it would be incorrect to consider this a "channel-scale flow circulation" or "cell" as there is no evidence (Figure 1b) that the flow completes even one half of a helix. Although measurements of turbidity were not possible in 2004, Figure 1b shows pockets of turbid water upwelling into clear water very soon after the junction, and this may be associated with either this increased shear or turbulence associated with large sand dunes. In morphological terms, the shape of the bed is similar at $x/W = 0.272$ and 0.539 (although the

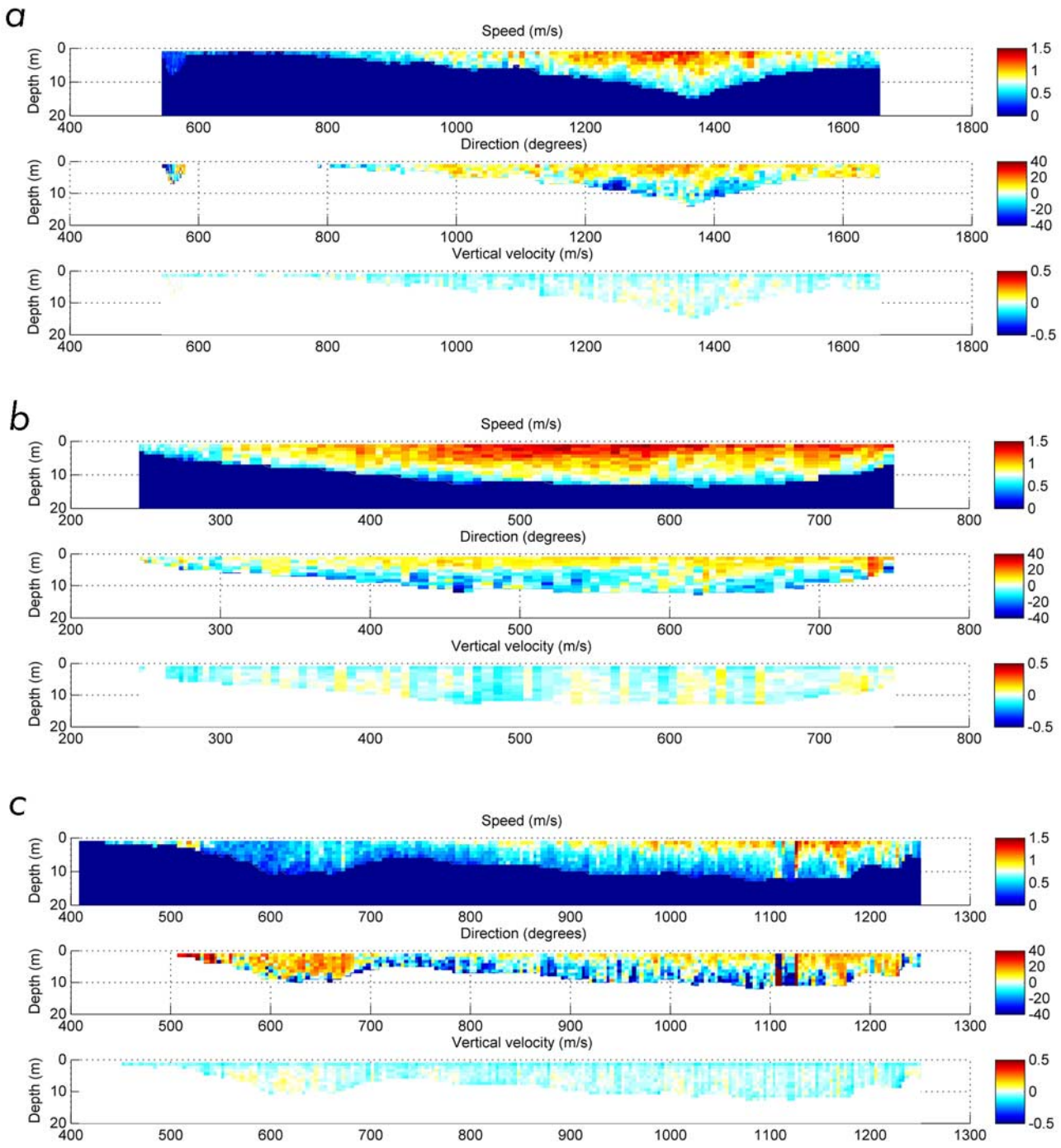

Figure 7. Transect surveys for 2004 of flow speed velocity, flow direction (with respect to transects oriented to give zero net cross-stream discharge, positive toward the Río Paraguay and negative toward the Río Paraná), and vertical velocity (positive upward). Data are presented for three transects (see Figure 2 for locations), i.e., (a) $x/W = 0.272$, (b) $x/W = 0.539$, and (c) $x/W = 0.712$. Each cross section is viewed looking downstream, i.e., distance is measured from the true left.

surveyed length of the transect at $x/W = 0.539$ is shorter). In summary, although comparison of the 2005 transects with 2004 is restricted by the lack of suspended sediment data, the transect data shown in Figure 7 indicate channel-scale flow patterns at a time when there was exceptionally rapid mixing. In these larger rivers, these data suggest that, for such rapid mixing to occur, conditions that allow such scales of transfer must develop.

5. Discussion

[22] From the above evidence, it is possible to evaluate the contribution of near-field processes to river mixing in

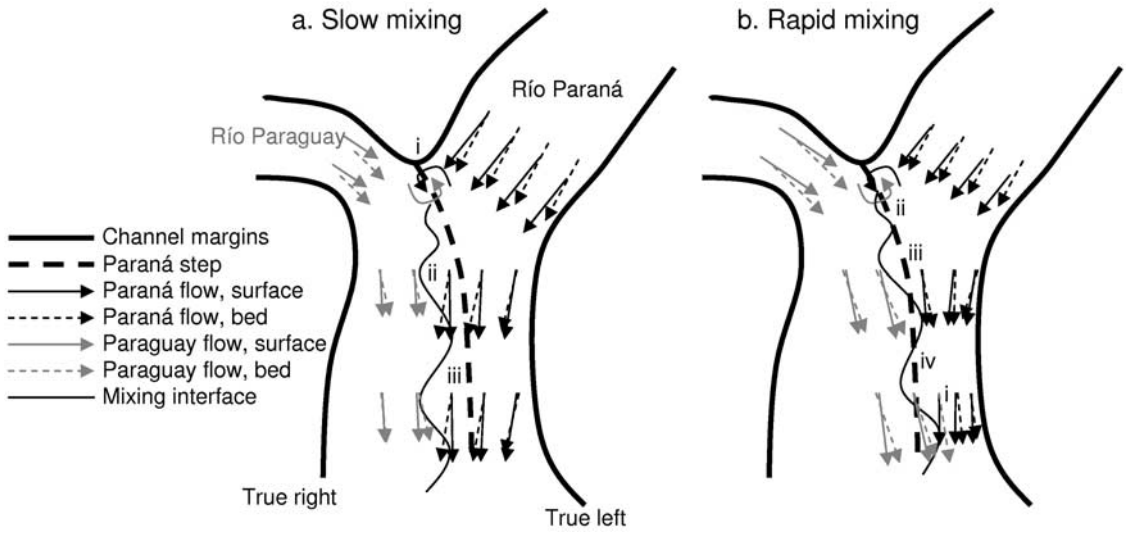

Figure 8. Schematic diagram to illustrate the near-field flow processes during (a) slow mixing and (b) rapid mixing.

relation to the semitheoretical analysis outlined at the beginning of this paper. A schematic diagram of the main features of flow when mixing is both slow and rapid is given in Figure 8. First, we have quantified the impacts on mixing created by the shear instabilities (Figure 8a(i)) that formed between the Río Paraguay and Río Paraná, close to the junction corner. In 2005, these appeared to enhance mixing close to the junction corner, but this mixing decayed rapidly with distance downstream, and was accompanied by a rapid decay in the association between lateral flow velocity and lateral suspended sediment concentration (Figure 3). When the downstream transects are considered (Figure 5), there was no clear difference in flow velocity, and hence shear, although there was a relatively diffuse transition at both $x/W = 0.539$ and 0.712 between flow on the right of the channel moving toward the Río Paraná and on the left moving toward the Río Paraguay (Figure 8a). This boundary was near vertical at $x/W = 0.539$ but was angled at $x/W = 0.712$, and in marked contrast to the suspended sediment distributions (Figure 5). In 2005, water from the Río Paraguay extended underneath that of the Río Paraná. However, the horizontally angled plane of shear we measured when mixing was more rapid in 2004 (Figure 7) was not present in 2005 (Figure 5). The absence of any sort of *shear* layer, despite the presence of a *mixing* layer, is commonly observed at small river confluences [e.g., *Rhoads and Sukhodolov*, 2001]. Downstream of $x/W = 0.272$, the transect-integrated lateral flux was commonly 2 orders of magnitude lower than the transect-integrated downstream flux. Consideration of the postconfluence width and position of the mixing interface in 2005 (Figure 1), suggests about 1.8 km of lateral transfer is needed for complete lateral mixing. However, if the lateral flux remains constant at 2 orders of magnitude less than the downstream flux, the downstream length required for mixing must be at least ~180 km. This is a similar order of magnitude to that observed in the case of slow mixing in 2005. Thus, in the absence of significant channel-scale circulation, the turbulence-driven mixing processes appear to result in a lateral transfer of momentum that is insufficient to cause significant mixing in the near field. While turbulence-related shear leads to a local increase in mixing rates close to the junction, a rapid decay in shear between the contributing flows is associated with a rapid decay in mixing rate.

[23] Second, we have measured the near-field conditions when mixing of the confluent flows can be very rapid. In 2004, this was in only $\sim 8W$, which is significantly more rapid than is typically observed in the rapid mixing of small rivers [*Gaudet and Roy*, 1995]. Rapid mixing appears related to the extension of turbid water from the Río Paraguay throughout the flow width (Figure 1b) and underneath water from the Río Paraná (Figure 8b(i)). This was accompanied by water moving at the surface from the Río Paraná toward the Río Paraguay (Figure 7), although clear Río Paraná water never reaches the true right bank (Figure 1b) and so never completes even half of a full helix. Instead, this circulation sets up a very strong, horizontally angled, plane shear layer that was accompanied (e.g., Figure 1b) by the upwelling of more turbid Río Paraguay water into the Río Paraná. The presence of an angled shear or mixing interface discriminates the case of slow mixing in 2005 from the more rapid mixing in 2004. In terms of the large river studied here, mixing in 2005 was dominated by turbulence-driven processes associated with a near-vertical shear layer forming close to the junction corner, but resulted in slow mixing rates. In 2004, turbulence-driven mixing associated with a near-horizontal plane shear layer resulting from one river flowing under the second across the full channel width, resulted in much more rapid mixing.

[24] The key question that emerges is why does this channel-scale circulation pattern appear in the case of rapid mixing and why is it absent when mixing is slow? This is a particularly important question because both empirical evidence and theoretical analysis suggest that the large width to depth ratio in wide rivers may impede the formation of coherent channel-wide secondary flow cells [*McLelland et al.*, 1999]. For example, *Parsons et al.* [2008] found that for

a braid bar confluence-diffluence in the Río Paraná, channel-scale secondary circulation cells were absent. They attributed this to the high channel width:depth ratio, which allowed the effects of form roughness to become dominant. In theory, the magnitudes of the terms in a force balance analysis of confluent flows [e.g., *Bradbrook et al.*, 2000] vary as a function of width, depth and velocity. Classic relationships in downstream hydraulic geometry show that the rate of increase of width (with increasing discharge and hence distance downstream) is commonly much greater than the rate of increase of either depth or velocity. Additionally, if the observation of *Leopold and Wolman* [1960] that the radius of curvature is a linear function of channel width holds for larger rivers, the analysis of *Bradbrook et al.* [2000] shows that the low rate of increase of velocity with distance downstream should reduce the magnitude of pressure-driven channel-scale circulation. Thus, the presence of such channel-scale circulation is surprising and we explain this in terms of the interaction between bed discordance, downstream topographic forcing and the momentum ratio between the confluent channels.

[25] Bed discordance has been shown to have a critical effect on the formation of flow structures in small river confluences [e.g., *Best and Roy*, 1991; *Biron et al.*, 1993, 1996]. Figure 2 shows that the Río Paraná enters the confluence at about half the depth of the Río Paraguay, resulting in a morphological step between the rivers (Figure 8b(ii)). Before this morphological step curves gradually to become aligned with the postconfluence channel (Figure 8b(iii)), it should allow turbid Río Paraguay water to move underneath the Río Paraná as the Río Paraná flows over the step. This situation certainly appears to be occurring in 2005, when we have reliable data on turbidity, with a tongue of turbid water extending partially across the channel at the bed. However, in itself the observation of the influence of bed discordance does not explain why the same river with the same discordance has channel-scale circulation at one time period and not at another. In the case of slow mixing, with no channel-scale circulation, the effect of bed discordance appears to be countered by the effects of downstream topographic forcing associated with the face of the step, as it curves to become aligned with the Río Paraná (Figure 2). In 2005, when there was no channel-scale circulation, the changing orientation of the step had two effects. First, it appeared to steer the Río Paraguay flow, throughout its depth, toward the Río Paraguay side of the channel (Figure 8a(iii)), and this served to keep the turbid Río Paraguay water on the right-hand side of the postconfluence channel. Second, the morphological step established a reverse bed gradient that reduced the ability of the more turbid Río Paraguay water to move toward the Río Paraná at the bed. Thus, the effect of the changing step direction in the postconfluence channel was to *prevent* the mixing interface migrating toward the Río Paraná and to work against the effect of the bed discordance in its influence on the transfer of more turbid water toward the Río Paraná. This process could also be exacerbated by form roughness and stronger steering of the flow by the bed as the flow shallows over the step. Indeed, the presence of a near-uniform flow direction throughout the vertical would be significant as it is exactly what *Parsons et al.* [2008] report for a confluence associated with a braid bar, further downstream in the same river. *Parsons et al.* [2008] reasoned the high *W*:*d* ratio allowed the effects of bed roughness to be transmitted throughout the flow depth and hence permitted the effects of topographic steering of the flow at the bed to become dominant over any larger channel-scale circulations.

[26] Given that the flow depth was slightly lower in 2004 when channel-scale circulation was present, the question that arises is why this form roughness did not prevent channel-scale circulation from developing. The answer appears to lie with the increased momentum of the Río Paraguay in 2004, as compared with the Río Paraná, as expressed by the momentum ratio (Paraná:Paraguay; equation (2); Table 2): $\sim$1.8 in 2004 (channel-scale circulation present) and $\sim$3.6 in 2005 (channel-scale circulation absent), with the prime factor for this difference being a higher discharge, rather than a higher density, in the Río Paraguay in 2004. Laboratory [*Best*, 1987, 1988], field [*Rhoads*, 1996; *Rhoads and Kenworthy*, 1998; *Rhoads and Sukhodolov*, 2001] and numerical [*Bradbrook et al.*, 1998, 2001] studies of small river confluences have shown that the momentum ratio exerts a critical effect on the interaction between two confluent streams and also conditions the effects of discordance upon flow structure formation [*Bradbrook et al.*, 1998, 2001]. Although the Río Paraná has a higher discharge than the Río Paraguay in both 2004 and 2005, it can be speculated that the higher momentum of the Río Paraguay in the case of rapid mixing (2004) allowed greater lateral expansion of the Río Paraguay into the Río Paraná through: (1) in the Río Paraguay, a reduction in the relative magnitude of topographic forcing compared with the downstream momentum terms, as a result of the higher transect-averaged flow velocity in the Paraguay and (2) in the Río Paraná, reduced resistance to deflection as a result of relatively lower transect-averaged velocity (Table 2). It thus appears that, with the lower 2004 momentum ratio, the increased lateral advection of the momentum of the Río Paraguay fluid at the bed was able to overcome the reverse topographic forcing of the bed that results from the extension of the morphological step on the left hand side of the channel (Figure 8b(iv)). Thus, the bed discordance, which allows Río Paraguay water to move underneath the Río Paraná, as well as the greater relative momentum of the Río Paraguay, combine to drive the rapid movement of turbid water further across the full postjunction width, and result in both channel-scale circulation and mixing within a very short distance downstream. This may have been aided by the higher density of the Río Paraguay in 2004, associated with the higher suspended sediment concentration. The possible contribution of density differences to near-field mixing remains an issue that needs further research.

[27] This discussion provides detailed evidence of how near-field processes can lead to the formation of channel-scale flow structures at the junction of a large river, which appears to have resulted in an exceptionally rapid rate of mixing in 2004. However, since we presently only possess measurements at two momentum ratios, development of a predictive model from our data for estimating how near-field effects reduce downstream mixing lengths is not possible. Similarly, measurements at a greater number of momentum ratios are required to assess whether there is a gradual relationship between the change in momentum ratio and mixing length, or a critical threshold in the momentum

ratio that discriminates between very rapid mixing and much slower mixing. Field data may help here, but measuring such large rivers is time consuming, expensive and logistically difficult, and the momentum ratio cannot be controlled in the way it can in physical or numerical models. Since a critical variable appears to be the high *W*:*d*, it is unlikely that physical modeling can address the full range of required boundary conditions, and thus it will be essential to reproduce and extend the type of modeling approach developed by *Bradbrook et al.* [2001] for high values of *W*:*d*, in order to help to understand and to predict how momentum ratio interacts with bed discordance to determine downstream mixing rates. *Bradbrook et al.* [2001] designed numerical experiments for small river junctions in which the effects upon flow structures of different combinations of junction asymmetry, junction angle, momentum ratio and depth ratio (i.e., level of bed discordance) were simulated numerically. These experiments showed those combinations of conditions which produced the strongest channel-scale secondary circulation and hence the most rapid mixing rates. Following from the conclusions of *Bradbrook et al.* [2000], development of a simple predictive model for near-field impacts may not be possible because these impacts are sensitively dependent upon the precise combination of driving variables, such as momentum ratio and local junction bed morphology. We have very few detailed measurements of three-dimensional geometry and flow processes in the World's largest rivers, and only one detailed measurement of the bed morphology of a large river confluence (Figure 2). This restricts the extent to which we can speculate on the role that is played by bed geometry. However, since river width scales with bankfull discharge [*Leopold and Maddock*, 1953], and bankfull discharge scales with basin area [*Emmett*, 1975], as rivers become larger there is a greater probability that they will differ in terms of their discharge because of: (1) differences in basin area and (2) basin areas that capture different climatic regimes and topographic and lithological terrains, and hence experience different discharge fluctuations within and between years. If rapid mixing requires particular values of momentum ratio (in relation to a particular bed geometry), then the extent to which these values are obtained will be controlled by time-varying, basin-scale processes. If we apply an ergodic hypothesis to the data shown in Table 1, the required momentum ratios are produced for only a very small proportion of time, and thus rapid mixing may be expected to occur rarely.

6. Conclusions

[28] The present paper has shown that the distances required for mixing at large river junctions are often long, but can be very short, even within the same junction at different times. When mixing at the confluence of the Río Paraná and Río Paraguay required a longer downstream distance, more than 100 multiples of postconfluence width, near-field mixing was restricted to instabilities generated along the near-vertical shear layer between the two flows. In this case, the associated lateral flux decayed rapidly downstream because of lessening of turbulent shear between the two confluent flows. Such slow mixing was also associated with an absence of channel-scale circulation. However, when mixing occurred in a strikingly short distance downstream, the primary cause was the presence of channel-scale flow circulation in the near field at the confluence, which allowed water from one river to penetrate fully underneath the other flow. In this case, the reasons for this circulation are a change in the momentum ratio, in relation to the effects of both bed discordance at the confluence and the way in which river morphology downstream of the junction either enhances or slows mixing. The latter is aided by the high *W*:*d* ratio, which allows easy transmission of bed topographic forcing throughout the complete flow depth. Our results present the first detailed data concerning the dynamics of mixing at a large river junction, and highlight the clear need for further investigation, most fruitfully combining field study with numerical simulations, to explore the fuller range of boundary conditions that may lead to slow or rapid mixing at these key nodes in fluvial networks.

[29] **Acknowledgments.** This research was supported by grants NER/A/S/2001/00445 and NER/B/S/2003/00243 from the U.K. Natural Environment Research Council and a Joint International Project from the Royal Society. The staff of CECOAL-CONICET (Corrientes, Argentina), and in particular Lolo Roberto, Rocque Negro, and Luis Bonnetti, provided crucial field support. Two anonymous reviewers, Yarko Nino, an Associate Editor, and the Editor provided invaluable suggestions on an earlier draft of this manuscript.

References

Best, J. L. (1987), Flow dynamics at river channel confluences: Implications for sediment transport and bed morphology, in *Recent Developments in Fluvial Sedimentology, Special Publications*, vol. 39, edited by F. G. Ethridge, R. M. Flores, and M. D. Harvey, pp. 27–35, Soc. of Econ. Paleontol. and Mineral, Tulsa, Okla.

Best, J. L. (1988), Sediment transport and bed morphology at river channel confluences, *Sedimentology*, *35*, 481–498, doi:10.1111/j.1365-3091.1988.tb00999.x.

Best, J. L., and A. G. Roy (1991), Mixing-layer distortion at the confluence of channels of different depth, *Nature*, *350*, 411–413, doi:10.1038/350411a0.

Biron, P., A. G. Roy, J. L. Best, and C. J. Boyer (1993), Bed morphology and sedimentology at the confluence of unequal depth channels, *Geomorphology*, *8*, 115–129, doi:10.1016/0169-555X(93)90032-W.

Biron, P., J. L. Best, and A. G. Roy (1996), Effects of bed discordance on flow dynamics at open channel confluences, *J. Hydraul. Eng.*, *122*, 676–682, doi:10.1061/(ASCE)0733-9429(1996)122:12(676).

Bradbrook, K. F., P. Biron, S. N. Lane, K. S. Richards, and A. G. Roy (1998), Investigation of controls on secondary circulation and mixing processes in a simple confluence geometry using a three-dimensional numerical model, *Hydrol. Processes*, *12*, 1371–1396, doi:10.1002/(SICI)1099-1085(19980630)12:8<1371::AID-HYP620>3.0.CO;2-C.

Bradbrook, K. F., S. N. Lane, and K. S. Richards (2000), Numerical simulation of three-dimensional time-averaged flow structure at river channel confluences, *Water Resour. Res.*, *36*, 2731–2746, doi:10.1029/2000WR900011.

Bradbrook, K. F., S. N. Lane, K. S. Richards, P. Biron, and A. G. Roy (2001), Role of bed discordance at asymmetrical open-channel confluences, *J. Hydraul. Eng.*, *127*, 351–368, doi:10.1061/(ASCE)0733-9429(2001)127:5(351).

Brown, G. L., and A. Roshko (1974), On density effects and large structure in turbulent mixing layers, *J. Fluid Mech.*, *64*, 775–816, doi:10.1017/S002211207400190X.

Dinehart, R. L., and J. R. Burau (2005), Averaged indicators of secondary flow in repeated acoustic Doppler current profiler crossings of bends, *Water Resour. Res.*, *41*, W09405, doi:10.1029/2005WR004050.

Emmett, W. W. (1975), The channels and waters of the upper Salmon River area, Idaho, *U.S. Geol. Surv. Prof. Pap. 870A*, U.S. Geol. Surv., Reston, Va.

Fischer, H. B., E. J. List, R. C. Y. Koh, J. Imberger, and N. H. Brooks (1979), *Mixing in Inland and Coastal Waters*, 483 pp., Elsevier, New York.

Gaudet, J. M., and A. G. Roy (1995), Effect of bed morphology on flow mixing length at river confluences, *Nature*, *373*, 138–139, doi:10.1038/373138a0.

Kennedy, B. A. (1984), On Playfair's law of accordant junctions, *Earth Surf. Processes Landforms*, *9*, 153–173, doi:10.1002/esp.3290090207.

Krouse, H. R., and J. R. Mackay (1971), Application of $H_2^{18}O/H_2^{16}O$ abundances to the problem of lateral mixing in the Liard-Mackenzie river system, *Can. J. Earth Sci.*, *8*, 1107–1109.

Lane, S. N., K. F. Bradbrook, K. S. Richards, P. M. Biron, and A. G. Roy (2000), Secondary circulation cells in river channel confluences: Measurement artefacts or coherent flow structures?, *Hydrol. Processes*, *14*, 2047–2071, doi:10.1002/1099-1085(20000815/30)14:11/12<2047::AID-HYP54>3.0.CO;2-4.

Leopold, L. B., and T. Maddock Jr. (1953), The hydraulic geometry of stream channels and some physiographic implications, *U.S. Geol. Surv. Prof. Pap. 252*, U.S. Geol. Surv., Reston, Va.

Leopold, L. B., and M. G. Wolman (1960), River meanders, *Geol. Soc. Am. Bull.*, *71*, 769–794, doi:10.1130/0016-7606(1960)71[769:RM]2.0.CO;2.

Mackay, J. R. (1970), Lateral mixing of the Laird and Mackenzie rivers downstream from their confluence, *Can. J. Earth Sci.*, *7*, 111–124.

Matsui, E., F. Salati, I. Friedman, and W. L. F. Brinkman (1976), Isotopic hydrology of the Amazonia: 2. Relative discharge of the Negro and Solimões rivers through 18° concentrations, *Water Resour. Res.*, *12*, 781–785, doi:10.1029/WR012i004p00781.

McLelland, S. J., P. J. Ashworth, and J. L. Best (1996), The origin and downstream development of coherent flow structures at channel junctions, in *Coherent Flow Structures in Open Channels*, edited by P. J. Ashworth et al., pp. 459–490, John Wiley, New York.

McLelland, S. J., P. J. Ashworth, J. L. Best, J. Roden, and G. J. Klaassen (1999), Flow structure and transport of sand-grade suspended sediment around an evolving braid bar, Jamuna River, Bangladesh, *Spec. Publ. Int. Assoc. Sedimentol.*, *28*, 43–57.

Mosley, M. P. (1976), An experimental study of channel confluences, *J. Geol.*, *84*, 535–562.

Muste, M., K. Yu, and M. Spasojevic (2004), Practical aspects of ADCP data use for quantification of mean river flow characteristics; Part I: Moving-vessel measurements, *Flow Meas. Instrum.*, *15*, 1–16, doi:10.1016/j.flowmeasinst.2003.09.001.

Parsons, D. R., J. L. Best, S. N. Lane, O. Orfeo, R. J. Hardy, and R. Kostaschuk (2008), Form roughness and the absence of secondary flow in a large confluence-diffluence, Paraná River, Argentina, *Earth Surf. Processes Landforms*, in press.

Rhoads, B. L. (1996), Mean structure of transport-effective flows at an asymmetrical confluence when the main stream is dominant, in *Coherent Flow Structures in Open Channels*, edited by P. J. Ashworth et al., pp. 491–517, John Wiley, New York.

Rhoads, B. L., and S. T. Kenworthy (1995), Flow structure at an asymmetrical stream confluence, *Geomorphology*, *11*, 273–293, doi:10.1016/0169-555X(94)00069-4.

Rhoads, B. L., and S. T. Kenworthy (1998), Time-averaged flow structure in the central region of a stream confluence, *Earth Surf. Processes Landforms*, *23*, 171–191, doi:10.1002/(SICI)1096-9837(199802)23:2<171::AID-ESP842>3.0.CO;2-T.

Rhoads, B. L., and A. N. Sukhodolov (2001), Field investigation of three-dimensional flow structure at stream confluences: 1. Thermal mixing and time-averaged velocities, *Water Resour. Res.*, *37*, 2393–2410, doi:10.1029/2001WR000316.

Rogers, M. M., and R. D. Moser (1992), The three-dimensional evolution of a plane mixing layer: The Kelvin-Helmholtz rollup, *J. Fluid Mech.*, *243*, 183–226, doi:10.1017/S0022112092002696.

Rutherford, J. (1994), *River Mixing*, Wiley, Chichester, U.K.

Stallard, R. F. (1987), Cross-channel mixing and its effect on sedimentation in the Orinoco River, *Water Resour. Res.*, *23*, 1977–1986, doi:10.1029/WR023i010p01977.

Sukhodolov, A. N., and B. L. Rhoads (2001), Field investigation of three-dimensional flow structure at stream confluences: 2. Turbulence, *Water Resour. Res.*, *37*, 2411–2424, doi:10.1029/2001WR000317.

Szupiany, R. N., M. L. Amsler, J. L. Best, and D. R. Parsons (2007), Comparison of fixed- and moving-vessel flow measurements with an aDp in a large river, *J. Hydraul. Eng.*, *133*, 1299–1309, doi:10.1061/(ASCE)0733-9429(2007)133:12(1299).

Weibezahn, F. H. (1983), Downstream natural mixing of water from the Orinoco, Atabapo and Guaviare rivers, *Eos Trans. AGU*, *64*(45), 699.

Winant, C. D., and F. K. Browand (1974), Vortex pairing: The mechanism of turbulent mixing layer growth at moderate Reynolds numbers, *J. Fluid Mech.*, *63*, 237–255, doi:10.1017/S0022112074001121.

Yorke, T. H., and K. A. Oberg (2002), Measuring river velocity and discharge with acoustic Doppler profiler, *Flow Meas. Instrum.*, *13*, 191–195, doi:10.1016/S0955-5986(02)00051-1.

J. L. Best, Department of Geology, University of Illinois at Urbana-Champaign, 245 Natural History Building, 1301 West Green Street, Urbana, IL 61801, USA.

R. J. Hardy and S. N. Lane, Department of Geography, Durham University Science Laboratories, South Road, Durham DH1 3LE, UK. (s.n.lane@durham.ac.uk)

R. A. Kostaschuk, Department of Geography, University of Guelph, Guelph, ON, Canada, N1G 2W1.

O. Orfeo, Centro de Ecología Aplicada del Litoral, Consejo Nacional de Investigaciones Cientificas y Tecnicas, CC 291, 3400, Corrientes, Argentina.

D. R. Parsons, School of Earth and Environment, University of Leeds, Environment Building, Leeds LS2 9JT, UK.